

EUROPEAN ORGANIZATION FOR NUCLEAR RESEARCH

Proposal to the ISOLDE and Neutron Time-of-Flight Committee

Study of the radiative decay of the low-energy isomer in ^{229}Th

May 11, 2020

S. Kraemer¹, K. Beeks², M. Block³, T. Cocolios¹, J.G. Correia⁴, S. Cottenier⁵, H. De Witte¹,
K. Dockx¹, R. Ferrer¹, S. Geldhof⁶, U. Köster⁷, M. Laatiaoui⁸, R. Lica⁴, P.-C. Lin⁹,
V. Manea¹⁰, J. Moens⁹, I. Moore⁶, L. M. C. Pereira⁹, S. Raeder³, M. Reponen⁶, S. Rothe⁴,
T. Schumm², B. Seiferle¹¹, S.Sels¹, P.G. Thirolf¹¹, P. Van Den Bergh¹, P. Van Duppen¹,
A. Vantomme⁹, M. Verlinde¹, E. Verstraelen¹, U. Wahl¹²

¹ *Institute for Nuclear and Radiation Physics, KU Leuven, Belgium*

² *Institute of Atomic and Subatomic Physics, Vienna University of Technology, Austria*

³ *GSI Helmholtzzentrum für Schwerionenforschung, Germany*

⁴ *ISOLDE-CERN, Switzerland*

⁵ *Center for Molecular Modelling, Ghent University, Belgium*

⁶ *Department of Physics, University of Jyväskylä, Finland*

⁷ *Institut Laue-Langevin Grenoble, France*

⁸ *Helmholtz-Institut Mainz, Germany*

⁹ *Quantum Solid State Physics, KU Leuven, Belgium*

¹⁰ *Institut de physique nucléaire d'Orsay, France*

¹¹ *Ludwig-Maximilians-Universität München, Germany*

¹² *Centro de Ciências e Tecnologias Nucleares, Universidade de Lisboa, Portugal*

Spokesperson: Piet Van Duppen piet.vanduppen@kuleuven.be

Contact person: Razvan Lica razvan.lica@cern.ch

Abstract:

A unique feature of ^{229}Th is its isomer with an exceptionally low excitation energy, proposed as a candidate for future nuclear optical clocks (1). Development of such a clock is however hindered by the uncertainty on the excitation energy and the lifetime of the radiative decay of this isomer. A spectroscopic measurement of the radiative decay is challenging due to the background conditions and has to-date not been successful. In this proposal, we present a spectroscopic measurement of the radiative decay based on a novel method to populate the isomer in the decay of ^{229}Ac after implantation into a calcium fluoride crystal (2). An experimental program studying the lattice incorporation of thorium in the crystalline environment and the vacuum-ultraviolet spectroscopy of the photons stemming from the radiative decay will contribute to the development of the next generation of ultra-stable clocks for metrology.

Requested shifts: 11 shifts



1 Physics motivation

In the mid 1970's, the existence of a low-energy nuclear isomer in ^{229}Th was proposed based on rotational bands observed in the alpha decay study of ^{233}U (3). Because of the unique nature of this isomer, situated only a few eV above the ground state, numerous experimental campaigns were initiated in an attempt to determine its precise excitation energy and decay characteristics (4, 5). Using an indirect method, i.e. measuring energy differences in γ -transitions feeding the ground or the isomeric state respectively, a value of $7.8 \pm 0.5\text{ eV}$ was proposed for the excitation energy making it accessible to laser excitation, a system so far unique in nature (6). Furthermore, an estimated relative radiative decay width of around $\Delta E/E \approx 10^{-19}$ opens up the possibility to develop an optical nuclear clock that could outperform existing atomic clock systems based on electronic shell transitions (1, 7). This can lead to new perspectives in ultra-high precision frequency quantum metrology with implications for both fundamental studies and technology, such as the search for possible time variations of the fundamental constants (see e.g. (4, 8, 9)). As the energy scales involving the nuclear excitation, the electron shell and the solid-state band structure are similar, different coupling schemes are possible representing a totally unexplored territory.

However, in spite of numerous efforts, it is only in 2016 that the existence of the ^{229m}Th isomer has been unambiguously proven by observing a signal induced by the internal electron conversion (IC) decay of neutral ^{229m}Th atoms. It was concluded that the excitation energy of the isomer is situated between 6.3 and 18.3 eV (10). The half-life value for the internal conversion (IC) decay channel of neutral ^{229m}Th was reported to be $7(1)\mu\text{s}$ (11).

Using the same set-up, laser spectroscopy studies on $^{229m}\text{Th}^{2+}$ ions were performed whereby the nuclear magnetic and quadrupole moments and spin were deduced (12). Recently, a precise determination of the energy of the second excited state of the ^{229}Th nucleus using synchrotron excitation, combined with previous transition energy measurements from excited states in ^{229}Th lead to a new, more restrained window between 2.5 to 8.9 eV for the isomer's energy (13). Parallel to these developments and analyzing the energy of the internal electron conversion signal from ^{229m}Th ions that decay in-flight, a new value for the energy of the isomer $8.28(17)\text{ eV}$, corresponding to $150(3)\text{ nm}$ photon wavelength in the case of radiative decay, was proposed in (14). All of these recent results place the isomer in an energy region below the band-gap of VUV transparent materials, paving the road towards an optical manipulation of the ^{229}Th isomer inside a solid-state environment, which is the starting point for this proposal.

The low excitation energy, comparable to the energy scale of the electronic band structure in combination with a factor of 10^9 difference in lifetime between internally converted and radiative decay, require a high degree of control over the chemical environment in order to

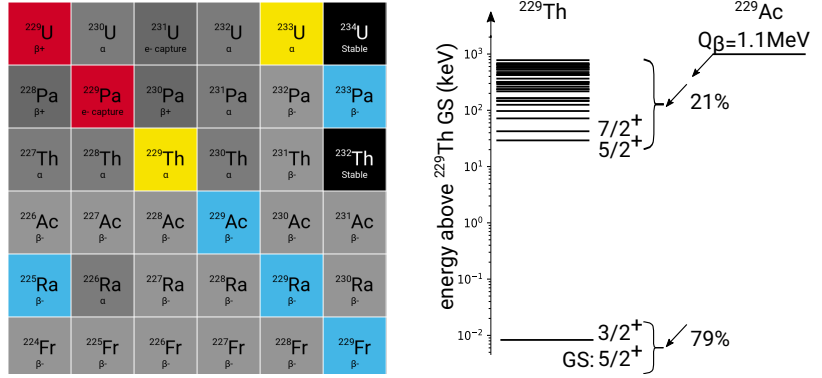


Figure 1: Left: Region of the nuclear chart around $A = 229, Z = 90$. The decay chains involving ^{229}Th are marked in color. Right: The β -decay of ^{229}Ac .

efficiently suppress the IC decay (15). The lattice position inside the solid-state matrix of a large band gap crystal determines the structure of energy bands and can lead to the appearance of additional electron energy bands within the band gap, which allow the internally converted decay (16). With an internal conversion factor of $\approx 10^9$, the radiative decay yield is strongly reduced (15). This challenge might explain the lack of success in observing the radiative decay despite numerous attempts. Additional difficulties arise from the small feeding of the isomer ^{229m}Th in the α -decay of ^{233}U , which is used in the majority of experiments to populate the isomer. Different mother nuclei decaying to and the nuclear structure of ^{229}Th are shown in figure 1.

In this proposal, we present an alternative method to populate the isomer using the β -decay of ^{229}Ac and propose a VUV-spectroscopic measurement of the radiative decay of ^{229m}Th using samples of ^{229}Ac beams implanted into large-band-gap crystals, leading to a measurement of its lifetime and energy at a 0.1 nm precision level (2). In the following sections, the advantages and results of preparatory studies (17) are presented and the feasibility of this proposal is discussed based on estimates of the expected signal strength and different background contributions.

2 Concept

This proposal consists of two parts:

1. **Emission channeling study of the Th position in the CaF_2 crystal lattice:** In order to assure the suppression of the internally converted decay channel of the isomer in a crystal environment, the thorium ion must occupy specific lattice positions. Using the emission channeling technique with ^{229}Ac and $^{231}\text{Ac}/^{231}\text{Th}$, the actinium and thorium lattice sites are studied and optimized (18).
2. **Vacuum ultraviolet spectroscopy of the radiative decay of ^{229}Th :** Laser ionized ^{229}Ac is implanted for a period of two half lives ($T_{1/2}(^{229}\text{Ac}) = 62.7 \text{ min}$) into a 50 nm thick calcium fluoride crystal. The sample is subsequently transferred under vacuum to an highly efficient vacuum ultraviolet (VUV) spectrometer, where photons from the radiative decay of the isomer populated in the β -decay of ^{229}Ac are detected.

Profiting from the availability of a number of neutron-rich actinium isotopes at ISOLDE, the following advantages for the study of the low-energy isomer in ^{229}Th using the β -decay of ^{229}Ac compared to the ^{233}U α -decay can be discerned:

- The feeding of the isomer is expected to be significantly higher compared to the alpha decay of ^{233}U , where only 2% of α -decays feed the isomer. From the β -decay scheme of ^{229}Ac as found in literature, 14% of the decays indirectly feed the $K^\pi = 3/2^+$ isomer via higher energy levels and γ -decay and 6% indirectly feed the $K^\pi = 5/2^+$ ground state (19). Due to the small excitation energy of the isomer, previous experiments could not distinguish between direct β -feeding of the isomer and the ground state, the sum amounting to 79% of all decays. With the direct feeding remaining unknown, the isomer population is increased by at least a factor of seven compared to ^{233}U .
- While the alpha decay of ^{233}U leaves the daughter nucleus with a recoil energy of 84 keV leading to re-implantation within the crystal, the recoil energy of the β -decay of ^{229}Ac is with maximum value of 6 eV smaller than typical displacement energies in calcium fluoride and the ^{229}Th daughter nucleus is expected to remain in the same lattice position.

- The half-life of 62.7 min of ^{229}Ac allows post-implantation annealing in the large band gap crystal in order to increase the fraction of ^{229}Ac nuclei in a substitutional lattice position inhibiting the internal conversion decay channel of the isomer. Density functional theory simulations have shown that the charge compensation mechanism for interstitial lattice positions can lead to additional electronic levels narrowing the band gap below the expected isomeric energy (16).
- The availability of a pure ion beam allows implantation into a large band gap crystal. Studies using ^{229}Ac created by neutron-activation were limited by the background contributions (20).
- The availability of the chain of β -emitters ^{231}Ac and ^{231}Th allows the instantaneous study of the lattice position of actinium and thorium after implantation and annealing using electron emission channeling.

Taking into account the outcomes of the preparatory studies in the framework of experiment I-198 (17), a concept for a study of the radiative decay is outlined.

3 Proposed experiment

3.1 Results from the feasibility study I-198 at ISOLDE

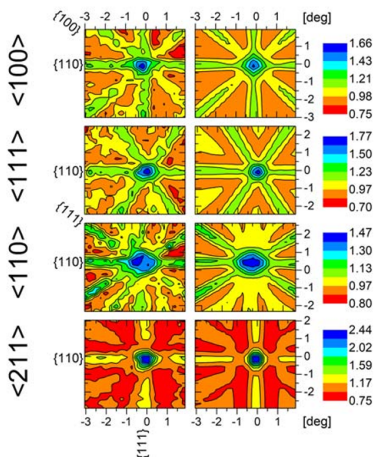


Figure 2: Emission channeling measurements of ^{229}Ac implanted CaF_2 (left) and numerical fit (right) in the vicinity of the $\langle 100 \rangle$, $\langle 111 \rangle$, $\langle 110 \rangle$ and $\langle 211 \rangle$ crystal axes.

Previous experiments at ISOLDE in the framework of I-198 allowed to exploit for the first time laser ionisation of actinium produced in a uranium carbide target with excitation from the $D_{3/2}$ ground state to the $4P_{3/2}^0$ excited state (438.58 nm) and towards an autoionizing state (456.15 nm). An additional contribution arises from surface-ionized ^{229}Ra and ^{229}Fr , decaying after implantation with a short half-life ($T_{1/2}(^{229}\text{Ra}) = 4$ min and $T_{1/2}(^{229}\text{Fr}) = 50$ s) to ^{229}Ac . Without further optimization, a total beam intensity of 10^6 particles per second has been observed at the experiment location (LA1). In-target production simulations indicate a gain of a factor of 50 in production for a thorium carbide target compared to uranium carbide.

The beam was used to perform gamma- and electron spectroscopy to verify, in an independent way, the decay scheme of ^{229}Ac as presented in a previous study (19). A beam of ^{229}Ac was retarded to 2 keV and implanted shallow below the surface of niobium and gold foils situated in a dedicated setup for efficient low-energy electron detection. The low-energy electrons escaping the implantation foil, were further accelerated by 500 eV and guided to a channeltron detector. This allowed for efficient detection of the conversion electron signal via the production of secondary electrons. The obtained γ -electron coincidence intensity was in agreement with what was expected from the decay scheme, giving confidence to the 14% feeding of the ^{229m}Th isomer in the beta decay of ^{229}Ac .

However, the low-energy conversion electrons stemming from the isomer were not observed. A possible explanation is the dependence of the lifetime of the converted decay on the chemical

environment, which might have shifted it out of the sensitivity range of our experimental setup which is between 4 μs and 50 μs including the 7(1) μs half life when implanted in a multichannel plate reported in literature (2, 11).

Additionally emission channeling experiments allowed to determine the lattice position of ^{229}Ac in calcium fluoride. Implanted into commercially available single crystals, the emission patterns shown in figure 2 were obtained. Preliminary analysis indicates that after implantation a fraction of 90 % remains in a substitutional lattice position. Since there are indications that the implanted depth profile is shallower than simulated by SRIM, which could reduce this fraction in the final analysis (ongoing), the count rate estimates made in this proposal are based on a worst-case scenario of 50 % substitutional fraction. Under the assumption that the β -decay towards ^{229}Th preserves the lattice position, a significant fraction sits in a favorable lattice position and allows the radiative decay of the isomer. Further studies using the β -emitter chain of ^{231}Ac , which were not possible during the I-198 experiment due to technical issues, are necessary to verify this assumption.

3.2 Lattice location using emission channeling

Emission channeling experiments will be performed, building on the preliminary results described above, with two main goals:

- A. To determine the optimal implantation and thermal annealing conditions in terms of maximizing the calcium-substitutional fraction and removing neighboring defects;
- B. To test the hypothesis that the thorium daughter nucleus inherits the actinium site.

Both aspects are crucial for the design and interpretation of the VUV spectroscopy experiments (section 3.3). The optimization of the implantation and annealing parameters (goal A) will be mostly based on ^{229}Ac experiments, as those described in the previous section, since the half-life (62.7 min) is sufficiently short to allow for fast measurements, and sufficiently long to allow for thermal annealing studies (typical annealing times of the order of 10 minutes). The experience accumulated with the I-198 feasibility study will allow us to perform detailed analysis in real-time, and therefore provide immediate input for the VUV experiments (section 3.3) which will take place in parallel. In order to test if the thorium daughter nucleus indeed inherits the actinium site (goal B), an additional set of emission channeling experiments will be performed using ^{231}Ac , which leaves the daughter nucleus with a comparable (and even slightly larger) recoil energy ($>13.5\text{ eV}$). With a half-life of 7.5 min, measurements on ^{231}Ac will be performed online in the EC-SLI setup, while the study of the ^{231}Th with a half-life of 25 h will be performed using the offline setups. These offline ^{231}Th experiments will also allow us to confirm the ^{229}Th results in terms of optimal implantation and annealing temperature (goal A). In order to perform these experiments, ^{231}Ac with a similar in-target production but a significantly shorter half-life needs to be extracted with an intensity of at least 10^5 pps.

Studying the lattice location of thorium in calcium fluoride and other large-bandgap materials is not only necessary to optimize the spectroscopy experiments (section 3.3) and for the interpretation of the resulting data, but also contributes to the evaluation of different doping techniques (doping during crystal growth vs. implantation) and delivers valuable information for the estimation of the achievable precision of the envisioned solid-state based optical clock due to the spread in hyperfine shifts for different lattice locations.

Contribution	Mean activity/rate	Decays/counts
β activity	318 kBq	$3.4 \cdot 10^{10}$ decays
isomer activity	21 kBq	$2.2 \cdot 10^8$ decays
collected photons at detector	10.5 Hz	$1.1 \cdot 10^5$ photons
detected isomer VUV photons	2.1 Hz	$2.3 \cdot 10^4$ counts
gamma interactions in PMT detector	17 mHz	184 counts
detected crystal γ radioluminescence	<5.7 mHz	< 62 counts
detected crystal β radioluminescence	1.3 mHz	15 counts
detected crystal α radioluminescence	30 nHz	\ll 1 counts
radiation induced counts at 150 ± 0.5 nm	0.024 Hz	262 counts
detector dark counts at 300 K	1 Hz	$1.1 \cdot 10^4$ counts

Table 1: Different signal and background contributions at 150 nm (with a spectrometer resolution of 1 nm for the radioluminescence contributions) in the vacuum ultraviolet spectroscopy experiment for 3 h following implantation of a 10^6 pps beam of ^{229}Ac beam for 2 h.

3.3 Vacuum-ultraviolet spectroscopy of the radiative decay of ^{229m}Th

The ^{229}Ac beam will be implanted at 30 keV into a calcium fluoride crystal within a 4 mm diameter beamspot. The mean implantation depth is 17 nm with a full-width half-maximum spread of 8 nm. The small volume of the crystal with dimensions $50 \text{ nm} \times 1 \text{ cm} \times 1 \text{ cm}$ grown on a silicon substrate allows to keep the background induced by radioluminescence limited. After an implantation time of 2 h ($T_{1/2} = 62.7$ min) with an implantation beam intensity of 10^6 pps, $4 \cdot 10^9$ ^{229}Ac nuclei are deposited in the crystal. Using a conservative estimate, 50 % of the ^{229}Ac nuclei as well as their ^{229m}Th daughters are assumed to occupy a substitutional lattice position and decay via the radiative decay channel. The remaining 50 % is assumed to be found in an interstitial lattice configuration and to decay via internal electron decay on a microsecond timescale.

After implantation the sample is placed close to the entrance slit of the VUV spectrometer to ensure optimum collection efficiency for the photons emitted in the radiative decay of the isomer. A VM180 grating spectrometer (Resonance Ltd, Canada) with a large numerical aperture of 0.49 (corresponding to F/1) and a slit width of $530 \mu\text{m}$ at 1 nm resolution is used in monochromator mode in combination with a detector based on a Hamamatsu R8487 photomultiplier tube with a quantum efficiency of 20 % at 150 nm. The cesium-iodide photocathode is sensitive between 115 nm and 195 nm, excluding the main contribution of radioluminescence, as discussed below. Different activities and background contributions are listed in table 1. Assuming the minimum isomer feeding of 14 %, corresponding to the indirect feeding known from literature, and a 2 h half-life of the isomer's radiative decay channel, the isomer's mean activity is 21 kBq and a total of $2.3 \cdot 10^8$ photons are emitted during 3 h following implantation.

The size of the entrance slit, adjustable during experiment, determines the working resolution of the spectrometer and allows to start the measurement at high photon collection efficiency with limited resolution to search for a signature to later improve the resolution up to the signal-to-background limit (with the spectrometer-intrinsic resolution limit at 0.1 nm). Using the model-specific quoted grating efficiency of 40 %, a conservative estimate leads to 0.05 % collection efficiency of photons behind the spectrometer. Taking into account the quantum efficiency of the PMT detector, a photon count rate of 2.1 Hz is expected.

The expected background consists of the temperature-dependent detector-intrinsic dark counts

and the radiation-induced counts, with typical conditions listed in table 1. Radiation induced background is created by radioluminescence of α -, β - and γ -radiation in the calcium fluoride crystal and interaction of γ -radiation with the PMT detector and its entrance window (10 % interaction probability). With an average energy of 360 keV, 110 eV is deposited on average by β -radiation in the calcium fluoride crystal. Using known scintillation properties of pure calcium fluoride, 1.17 photons are created per β -decay by β radiation and conversion electrons (21, 22). Most of the photons are located in a wavelength region between 220 nm and 350 nm in which the photocathode is not sensitive (23). The background at 150 nm is dominated by Cherenkov radiation, yielding 15 counts over 3 h in a 1 nm-wide spectral window. Gamma and X-ray photons from the decay of ^{229}Ac travel a mean distance of 355 nm in the crystal depositing on average 2.6 eV. Assuming a worst-case 100 % transformation of deposited energy into photons, and the relative spectral contribution of $3.1 \cdot 10^{-4}$ from (23), less than $1.8 \cdot 10^{-4}$ photons are created per β -decay in a 1 nm spectral region around 150 nm. Contributions by α -radioluminescence from the decay of ^{229}Th with a mean energy loss of 9 keV and a transformation rate into VUV photons of 1 % is negligible, as can be seen from table 1.

Next to a total of $2.3 \cdot 10^4$ detected photons emitted in the decay of the isomer, $1.1 \cdot 10^4$ uncorrelated random background counts originate from the detector-intrinsic dark counts and $2.6 \cdot 10^2$ background counts are radiation induced. The detector-intrinsic dark count rate can be reduced by a factor of 5 by cooling the detector to about -30°C where it reaches its optimal value (24).

Once a VUV signal is detected using the spectrometer with maximum resolution, a scan of the region of interest will be performed using a reduced slit width. The optimized spectral resolution will be based on the obtained signal to noise ratio. The β -delayed γ -decay of ^{229}Ac will be observed with germanium detectors and from a comparison of the time behavior of the gamma radiation and the VUV signal the half life of the isomer will be deduced.

Summary of requested shifts

- For the **optimization of extraction** of ^{229}Ac (previously extracted) and ^{231}Ac and for purity checks a total of **3 shifts** is requested.

Spectroscopy of the radiative decay and emission channeling measurements are preceded by an implantation period of 2 h.

- **Emission channeling** measurements for optimization of the implantation and annealing parameters require > 5 implantations. **2 shifts** split over several days are required.
- For **VUV spectroscopy** with ^{229}Ac , background checks and the lifetime measurement > 20 implantations are needed. **6 shifts** split over several days are required.

For the spectroscopy of the radiative decay and the study of lattice incorporation of thorium in calcium fluoride as developments towards an optical clock, we ask for a total of **11 shifts**.

References

1. E. Peik *et al.*, *Europhysics Letters* **61**, 181 (2003).
2. M. Verlinde *et al.*, *Physical Review C* **100**, 024315 (2019).
3. L. A. Kroger *et al.*, *Nuclear Physics A* **259**, 29–60 (1976).
4. E. Peik *et al.*, *Comptes Rendus Physique* **16**, 516–523 (2015).
5. P. G. Thirolf *et al.*, *Annalen der Physik* **531**, 1800381 (2019).

6. B. R. Beck *et al.*, LLNL-PROC-415170 (Lawrence Livermore Nat. Lab., 2009).
7. C. J. Campbell *et al.*, *Physical Review Letters* **108**, 120802 (2012).
8. V. Flambaum, *Phys. Rev. Lett.* **97**, 092502 (2006).
9. M. Safronova *et al.*, *Phys. Rev. Lett.* **121**, 213001 (2018).
10. L. von der Wense *et al.*, *Nature* **533**, 47–51 (2016).
11. B. Seiferle *et al.*, *Phys. Rev. Lett.* **118**, 042501 (2017).
12. J. Thielking *et al.*, *Nature* **556**, 321–325 (2018).
13. T. Masuda *et al.*, *Nature* **573**, 238–242 (2019).
14. B. Seiferle *et al.*, *Nature* **573**, 243–246 (2019).
15. F. F. Karpeshin *et al.*, *Physical Review C* **76**, 054313 (2007).
16. P. Dessovic *et al.*, *Journ. of Phys.: Cond. Matter* **26**, 105402, ISSN: 0953-8984 (2014).
17. P. Van Duppen *et al.*, INTC-I-198 (CERN, 2017).
18. U. Wahl *et al.*, *Nucl. Instr. and Meth. in Phys. Res. Section A* **524**, 245–256 (2004).
19. E. Ruchowska *et al.*, *Physical Review C* **73**, 044326 (2006).
20. Y. Shigekawa *et al.*, *Physical Review C* **100**, 044304 (2019).
21. V. Mikhailik *et al.*, *Nucl. Instr. and Meth. in Phys. Res. Section A* **566**, 522–525 (2006).
22. M. Moszyński *et al.*, *Nucl. Instr. and Meth. in Phys. Res. Section A* **553**, 578–591 (2005).
23. S. Stellmer *et al.*, *Scientific Reports* **5** (2015).
24. K. Beeks, private communication (2020).

Appendix

DESCRIPTION OF THE PROPOSED EXPERIMENT

The setup comprises: the EC-SLI online setup¹, two offline EC setups dedicated to emission channeling experiments and the travelling VUV spectroscopy setup.

Part of the	Availability	Design and manufacturing
Emission Channeling EC-SLI	<input checked="" type="checkbox"/> Existing	<input checked="" type="checkbox"/> To be used without any modification (EC-SLI setup at b.170-GHM) <input type="checkbox"/> To be modified
	<input type="checkbox"/> New	<input type="checkbox"/> Standard equipment supplied by a manufacturer <input type="checkbox"/> CERN/collaboration responsible for the design and/or manufacturing
Emission Channeling Offline	<input checked="" type="checkbox"/> Existing	<input checked="" type="checkbox"/> To be used without any modification (offline EC setups in b.508-R-008) <input type="checkbox"/> To be modified
	<input type="checkbox"/> New	<input type="checkbox"/> Standard equipment supplied by a manufacturer <input type="checkbox"/> CERN/collaboration responsible for the design and/or manufacturing
VUV Spectroscopy	<input type="checkbox"/> Existing	<input type="checkbox"/> To be used without any modification <input type="checkbox"/> To be modified
	<input checked="" type="checkbox"/> New	<input type="checkbox"/> Standard equipment supplied by a manufacturer <input checked="" type="checkbox"/> CERN/collaboration responsible for the design and/or manufacturing

HAZARDS GENERATED BY THE EXPERIMENT (if using fixed installation:) Hazards named in the document relevant for the fixed [COLLAPS, CRIS, ISOLTRAP, MINIBALL + only CD, MINIBALL + T-REX, NICOLE, SSP-GLM chamber, SSP-GHM chamber, or WITCH] installation.

Additional hazards:

Hazards	Emission Channeling (EC-SLI)	Emission Channeling (of-fine)	VUV Spectroscopy
Thermodynamic and fluidic			
Pressure	NA	NA	NA
Vacuum	1×10^{-6} mbar, 40 L	1×10^{-6} mbar, 5 L	1×10^{-6} mbar
Temperature	NA	NA	NA
Heat transfer	NA	NA	NA
Thermal properties of materials	NA	NA	NA
Cryogenic fluid	NA	NA	NA
Electrical and electromagnetic			
Electricity	230 V, 15 A	230 Vm 15 A	230 V, 15 A 3.5 kV (HPGe detector)
Static electricity	NA	NA	NA
Magnetic field	NA	NA	NA
Batteries	<input type="checkbox"/>	<input type="checkbox"/>	<input type="checkbox"/>

¹see <https://edms.cern.ch/document/1960302/1>

Capacitors	<input type="checkbox"/>	<input type="checkbox"/>	<input type="checkbox"/>
Ionizing radiation			
Target material [material]	CaF ₂	CaF ₂	CaF ₂
Beam particle type (e, p, ions, etc)	ions	ions	ions
Beam intensity	$< 5 \cdot 10^7$ pps	NA	$< 5 \cdot 10^7$ pps
Beam energy	30 keV	NA	30 keV
Cooling liquids	NA	NA	LN ₂ (HPGe detector)
Gases	NA	NA	N ₂
Calibration sources:	<input type="checkbox"/>	<input type="checkbox"/>	<input checked="" type="checkbox"/>
• Open source	<input type="checkbox"/>	<input type="checkbox"/>	<input type="checkbox"/>
• Sealed source	<input type="checkbox"/>	<input type="checkbox"/>	<input checked="" type="checkbox"/>
• Isotope	NA	NA	⁶⁰ Co
• Activity	NA	NA	100 kBq
Use of activated material:			
• Description	<input type="checkbox"/>	<input type="checkbox"/>	<input type="checkbox"/>
• Dose rate on contact and in 10 cm distance	NA	NA	NA
• Isotope	NA	NA	NA
• Activity	NA	NA	NA
Non-ionizing radiation			
Laser	class 2, 635 nm, 0.9 mW	NA	
UV light	NA	NA	120-400 nm (deuterium lamp)
Microwaves (300MHz-30 GHz)	NA	NA	NA
Radiofrequency (1-300 MHz)	NA	NA	NA
Chemical			
Toxic	NA	NA	NA
Harmful	NA	NA	NA
CMR (carcinogens, mutagens and substances toxic to reproduction)	NA	NA	NA
Corrosive	NA	NA	NA
Irritant	NA	NA	NA
Flammable	NA	NA	NA
Oxidizing	NA	NA	NA
Explosiveness	NA	NA	NA
Asphyxiant	NA	NA	NA
Dangerous for the environment	NA	NA	NA
Mechanical			
Physical impact or mechanical energy (moving parts)	NA	NA	NA
Mechanical properties (Sharp, rough, slippery)	NA	NA	NA
Vibration	NA	NA	NA
Vehicles and Means of Transport	NA	NA	NA
Noise			

Frequency	NA	NA	NA
Intensity	NA	NA	NA
Physical			
Confined spaces	NA	NA	NA
High workplaces	NA	NA	NA
Access to high workplaces	NA	NA	NA
Obstructions in passage-ways	NA	NA	NA
Manual handling	NA	NA	NA
Poor ergonomics	NA	NA	NA

Hazard identification:

Average electrical power requirements (excluding fixed ISOLDE-installation mentioned above):
 < 3 kW